Integration of Computations and Experiments for Flow Control Research With Undergraduate Students

Article *in* Computer Applications in Engineering Education · December 2010

DOI: 10.1002/cae.20278

4 authors, including:

Kelly Cohen
University of Cincinnati
214 PUBLICATIONS **1,035** CITATIONS

Integration of Computations and Experiments for Flow Control Research With Undergraduate Students

SELIN ARADAG,[1] KELLY COHEN,[2] CHRISTOPHER A. SEAVER,[3] THOMAS MCLAUGHLIN[3]

[1]TOBB *University of Economics and Technology, Ankara* 06560, *Turkey*

[2]*Department of Aerospace Engineering, University of Cincinnati, Cincinnati, Ohio* 45221-0070

[3]*Department of Aeronautics, United States Air Force Academy*, USAFA, *Colorado* 80840

Received 20 February 2008; accepted 21 August 2008

ABSTRACT: The methods and outcome of a senior undergraduate project related to the control of a turbulent cylinder wake flow using plasma actuators are summarized in this article. The study integrates computational fluid dynamics (CFD) with experimentation and combines fluid mechanics with flow control research, crossing the boundaries between engineering disciplines.Comput. Appl. Eng. Educ. © 2009 Wiley Periodicals, Inc. Comput Appl Eng Educ 18: 727–735, 2010; View this article online at wileyonlinelibrary.com; DOI 10.1002/cae.20278

Keywords: cylinder wake; CFD; flow control; plasma

INTRODUCTION

In traditional curricula undergraduate students take both numerical methods and laboratory courses; however, they usually work on already solved problems and simple test cases where the results are known a priori. As a result, involving undergraduate students in research has always been a challenge. It is usually common to engage graduate students in open ended research supported by funding agencies. At the United States Air Force Academy (an undergraduate institution), the Department of Aeronautics, gives senior students the chance to work on open ended problems as a part of world class research teams. The students are taught undergraduate CFD course and an experimental course that summarizes the measurements techniques and data analysis in addition to traditional undergraduate courses on Fluid Mechanics, Aerodynamics, etc. This article summarizes the methods and outcome of an undergraduate project supported by Air Force Office of Scientific Research (AFOSR) which is related to the control of flow at a turbulent wake of a circular cylinder using plasma actuators.

Aerodynamic drag caused by unsteady flows is an increasingly wide area of study. Whether it is applied to cars or aircraft, overcoming drag requires a significant amount of energy in transportation applications. The ability to reduce drag would decrease the need for energy sources, increase the range and endurance of vehicles, and lower the environmental stress caused by fossil fuel requirements. Specifically, bluff bodies on vehicles are substantial sources of aerodynamic drag. Creating unstable, turbulent flows, bluff bodies can create much of the drag, thus inefficiency, on a vehicle. Problems have encouraged research into methods to control the airflow around bodies and minimize their adverse effects.

A circular cylinder is a well-studied and documented benchmark for a bluff body wake problem. In a two-dimensional cylinder wake, self-excited oscillations in the form of periodic shedding of vortices are observed above a critical Reynolds number (*Re*) of approximately 40 [1]. This type of behavior is referred to as the von Kármán Vortex Street, named after Theodore von Kármán, who first discovered the phenomenon in 1911 [2]. These flow-induced nonlinear oscillations may lead to some undesirable effects associated with unsteady pressures such as fluid–structure interactions and lift/drag fluctuations. The Tacoma Narrows bridge catastrophe is attributed to fluid–structure interactions associated with the von Kármán Vortex shedding [2].

Active flow control of the cylinder wake offers researchers a simple, effective problem for developing and comparing different methodologies for feedback flow control. Many

Correspondence to S. Aradag (selinaradag@gmail.com).

examples exist in nature in which flow control is used to optimize fluid-dynamic forces for locomotion. Birds rely on control of unsteady vortices in their wake to optimize their cruise performance. Studies show that the greatest propulsive efficiency that can be attained by aerodynamic bodies, like birds, is for Strouhal number (St) ~ 0.2 [3]. Flow control can be divided into two categories. Control characterized by the addition of energy to the flow is active, while control attained by other means is considered passive. Additionally, flow control can be further subdivided into closed and open-loop control. Open-loop control is characterized by a system that has no feedback mechanism to control the actuator, while closed-loop control is typified as that which has a feedback mechanism to optimize the actuator input for flow control. Closed-loop active flow control offers one of the most promising methods for controlling the flow around bluff bodies, thereby mitigating the energy losses associated with drag. The essence of this flow control is the ability to use minimum energy to achieve maximum benefit in aerodynamic performance. This goal appears most promising when dealing with flow instability, as in the case of the von Kármán Vortex Street.

Recent research conducted at USAFA has pointed to the feasibility of using active flow control, especially applied to the vortex shedding in the wake behind a cylinder [4]. A necessary step in the employment of a functional actuation system is to determine an effective actuation mechanism. Experiments at USAFA have determined that a dielectric barrier discharge (DBD) plasma actuator is an effective method for achieving flow control [4]. When an AC current is applied between two electrodes, a layer of plasma is created, from the edge of the top, exposed electrode to the electrode buried beneath the dielectric material. The plasma adds a directed momentum to the flow and can even create an induced flow in the direction of the plasma. Because this actuator has no moving parts and no resonant frequency, it is an excellent actuator for inducing perturbations to the flow to achieve desired effects [4].

Further experiments have shown that lock-in is a prerequisite for appropriate modeling for flow control [5]. Lock-in is the ability of the shed vortices to match the frequency of the actuator. At higher actuator amplitudes (voltages in the case of the plasma actuator), the range of frequencies over which lock-in occurs is larger [4]. Establishing an area of which lock-in can be achieved using a plasma actuator and cylinder establishes an envelope of validity for the dynamic modeling of the flow, which forms the basis for further feedback controller/estimator design.

MAIN RESEARCH OBJECTIVES

The ultimate aim of this research program is to control the turbulent, unsteady wake behind a circular cylinder using closed loop flow control and utilizing plasma as an actuator to control the complex flow behind the cylinder. Both computational and experimental tools are used for this purpose. This particular research performed by undergraduate students (senior cadets from the Department of Aeronautics at USAFA) under the supervision of teaching and research faculty has two main objectives. First, experimental data is collected at the USAFA Low-Speed Wind Tunnel to validate the computational fluid dynamics (CFD) simulations of the model in order to integrate experimental efforts with CFD. Second, the operating range, or ''lock-in'' region, of amplitudes and frequencies over which plasma actuators successfully control the flow for the turbulent cylinder wake is determined to help further CFD efforts. Determination of the ''lock-in'' region for the plasma actuators to control turbulent flow and integrating CFD with experiments are crucial steps in closed loop flow control. Most importantly, this research gives senior undergraduate students the opportunity to work on real world research problems funded by important agencies in the area. During the three primary phases of this work (CFD, experimental validation, and plasma experiments), computers using several commercial and non-commercial software programs were widely used by students for data collection, plasma forcing and post-processing of data. Some main resources (books, main journal, and conference articles related to the subject) were provided to the students; however they performed a comprehensive literature survey on their own, which is an essential part of research. They were also shown a demo on how plasma changes the flow field over a circular cylinder in the laboratory, in order to let them visualize the flow better. Moreover, the study combines fluid dynamics research with flow control crossing boundaries between engineering disciplines.

COMPUTATIONAL METHODOLOGY

For the CFD simulations, the solver Cobalt from Cobalt Solutions, LLC, was used [6]. It is a commercial code which solves the compressible Navier–Stokes equations using a cell-centered finite volume approach applicable to arbitrary cell topologies (e.g., prisms, tetrahedra). It can achieve second order accuracy in both time and space. The three-dimensional flow was simulated using Large Eddy Simulations with no explicit subgrid scale model. The numerical dissipation of the code was relied upon to remove the energy from the resolved scales, mimicking the effect of turbulence at the subgrid level, an approach also used by Hansen and Forsythe [7]. At this Reynolds number, the attached boundary layer on the cylinder surface is laminar but the wake is fully turbulent.

The flow at Reynolds number (Re) of 20,000 was simulated at a Mach number (M) of 0.1. The length to diameter ratio (L/D) of the cylinder was 4. The diameter of the cylinder (D) was 2 m. Periodic boundary conditions were used on the computational surfaces at the cylinder ends. Modified Riemann invariants were used as a farfield boundary condition, and a no slip, adiabatic wall was employed for the cylinder surface.

A time step (Δt) of 1.152×10^{-3} seconds resulting in $\Delta tU/D = 0.04$ non-dimensional time steps was utilized. Time was non-dimensionalized by D/U, where D is the cylinder diameter and U is the free stream velocity. A time step study was also performed with half the time step to obtain time step independent computational results. The temporal resolution of the simulations was 250 time steps per von Kármán shedding cycle. Forty parallel processors were employed to perform the computations.

In order to increase the stability, an advection damping coefficient of 0.01 was used in the computations. Damping is any effect, either deliberately engendered or inherent to a system, that tends to reduce the amplitude of oscillations of an oscillatory system. Advection damping is an extra damping term that is added to the formulation of the advection term in the governing equations of flow in order to stabilize the solution.

No damping was used for diffusion. To provide the convergence of variables at every time step, three Newton sub-iterations were used. As an initial perturbation to trigger the unsteadiness in the flow simulations, the incoming flow was skewed by an angle of attack of 1°. This is an unsteady effect which was used as an initial condition only, that does not continue for the rest of the simulations.

The unstructured grid consists of prismatic cells clustered in the boundary layer and tetrahedral cells outside the boundary layer. It was generated by Gridtool/VGRID using the method of Morton et al. [8]. The minimum cell height is 1×10^{-3} m. When this is non-dimensionalized by the cylinder dimameter (D), the value is 5×10^{-4}. The average non-dimensional first cell height for the boundaries (y^{+}_{average}) is approximately 0.3. The grid has 879,603 cells.

The coordinate system used in the computations and the grid around the cylinder surface are shown in Figure 1. X is the streamwise direction and the y-axis is aligned with the cylinder axis. The origin is at the near end of the cylinder in the cylinder center. Figure 1 shows the surface grid, a plane normal to the cylinder axis, and a zoom-in near the surface.

A grid refinement study with a grid of 2.5 million cells was performed to obtain a grid-independent solution. The farfield boundaries are 20 diameters away from the cylinder surface. With a shedding frequency of $f = 3.47$ Hz, the calculated Strouhal number is 0.2 for this flow.

EXPERIMENTAL SET-UP

Experiments were performed for the same Reynolds number used in the computations ($Re = 20{,}000$) in the USAFA Low Speed Wind Tunnel (LSWT) to validate the main quantities related to the flow such as the Strouhal number, surface pressure distribution, drag coefficient and velocity distribution obtained from CFD simulations. This tunnel has a 0.9144 m $\times$ 0.9144 m test section with a usable velocity range of 3–35 m/s. A 0.09 m diameter cylinder spanned the entire height of the test section. Due to the relative sizes of the cylinder model and the LSWT, blockage corrections were performed in the analysis of data.

In order to verify the computational approach used in this study, surface pressure data around the cylinder were obtained using two different types of sensors, Validyne and Baratron. The Validyne pressure sensor has a range of ± 0.03 psid, an analog output of ± 10 V dc, and an accuracy of 0.25% of full scale. The sensors were connected to two different ports on the cylinder surface on centerplane and the cylinder was rotated with an increment of 10° to obtain pressure data along the whole circumference of the cylinder. Using two different sensors helped the validation of the results.

Single wire hot film probes were placed along the span of the model with the sensor axis being parallel with the cylinder axis. The hot film probes were positioned in line with the side of the cylinder, where the amplitude of the von Kármán Vortex Street induced oscillations is largest. They were initially placed 0.5 cylinder diameters (D) downstream of the cylinder to measure the frequency of the flow to compare to the CFD simulation data. Further data was taken to analyze the lateral velocity profile in the wake of the cylinder. The four hot film probes were placed $3D$ downstream of the cylinder and moved laterally from $z/D = +2.0$ to -2.0 in increments of 0.2 diameters.

For the plasma experiments, actuators were placed along the span at the 90° and 270° marks based on previous work done by McLaughlin et al. [4] indicating this as the optimal position. The actuators consisted of two strips of copper tape, one buried beneath the dielectric barrier and one on top as illustrated in the configuration in Figure 2. The copper tape is 0.010 cm thick and 0.64 cm wide, while the dielectric tape is 0.018 cm thick. Computer controlled voltage was amplified and transformers were used to increase the magnitude of the actuation voltage up to approximately 16 kV. The plasma formed atop the Teflon tape over the area of the buried electrode. Five layers of Teflon dielectric tape were used, as shown effective through the work of McLaughlin et al. [4] In this case however, the Teflon tape was only used on the front side of the cylinder to make room for the sensors on the back half as seen in Figure 2. A panel was cut from the downstream side of the cylinder for sensor placement. Sixteen pressure ports consisting of four rows of four ports were placed into this panel and a Scanivalve pressure multiplexer was fixed inside the cylinder with tubing connected to each of the 16 ports as illustrated in Figure 3.

The lock-in region of the plasma actuators was determined using a range of plasma actuation voltages for different actuation frequencies. The hot film rake mentioned earlier was placed $2.0D$ downstream of the cylinder and at $z = -0.5D$. Actuation frequencies ranging from $0.80f_0$ to $1.30f_0$, where f_0 is the vortex shedding frequency and voltages from approximately 1 to 16 kV were used to create an envelope where lock-in occurs. For each run, the unforced shedding frequency was computed using a fast Fourier Transform (FFT). During forcing, an FFT was used to determine if the actuation caused the shedding frequency to change from the unforced frequency to the actuation frequency. After identifying the lock-in region, the hot film rake was moved from the $z = -0.5D$ position to the $z = 0.5D$ position to test the symmetry of the lock-in region. Actuation frequencies for the symmetry test ranged from $0.86f_0$ to $1.25f_0$ at both 12 and 14 kV. All the measurements were performed by controlling the experiments using Labview computer software.

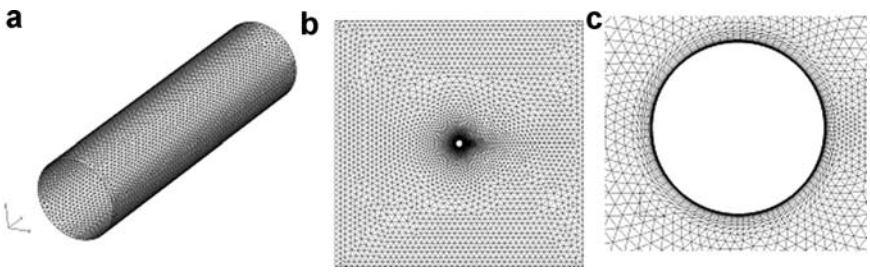

Figure 1 (a) Surface mesh, (b) mesh at the periodic boundary plane, and (c) zoom-in near the surface.

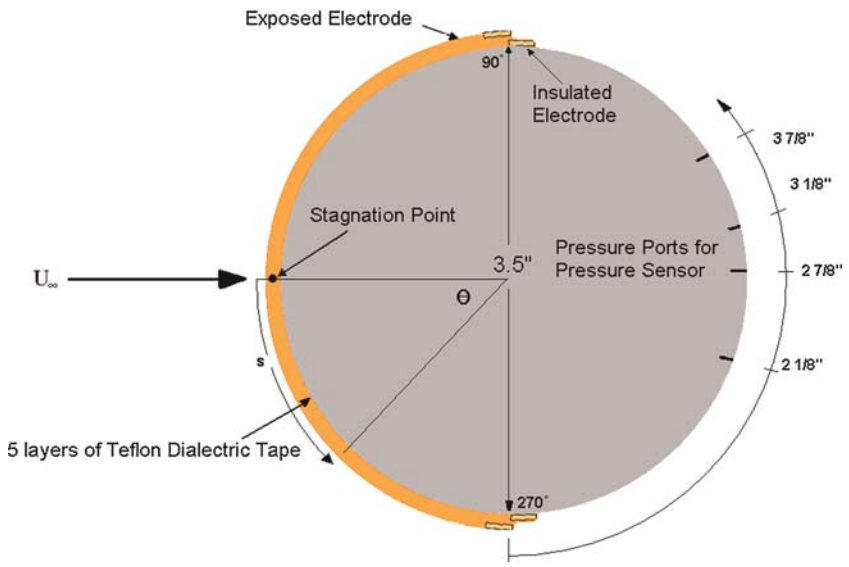

Figure 2 Top view of cylinder set-up. [Color figure can be viewed in the online issue, which is available at wileyonlinelibrary.com.]

POST-PROCESSING TOOLS

Excel and MATLAB programs were primarily used to process the data from all sensors. First, using the gains and offsets of the four hot film anemometers, and then a fourth order polynomial and its coefficients describing the calibration curve, the raw hot film voltages can be converted into velocities. Similarly, the data from the sensors could be directly converted from voltages to pressures. For both sensor types, the correlation between the voltage and pressure is linear. A master Excel file was used to keep track of all calculations and conversions. During testing, data was collected from the array of sensors using the data acquisition system and converted into an Excel spreadsheet format. The Excel files were then converted to a format more easily integrated into MATLAB using a macro. Much of the data had non-physical spikes which clouded the rest of the data. Using MATLAB, these spikes were removed and replaced with an average value from the rest of the data. Next, mean tunnel velocity was plotted to ensure that the conditions were relatively stable and data acquisition system was working. Data was filtered using a 5th order lowpass Butterworth digital filter with a 60 Hz cutoff from MATLAB and the function ''filtfilt.'' These filters cleaned up all of the high frequency noise. A MATLAB Fast Fourier Transform (FFT) was used to transform the data from the time domain to the frequency domain for analysis and was used to extract the frequency content from both the velocity and pressure data. Finally, a Welch averaged periodgram application, called ''pwelch'' in MATLAB, was used to normalize the FFT to present the results independent of sample size. In this way, findings for different trials could be compared on the same scale.

MATLAB was also used to organize and present the results of the wake velocity profile analysis. After the hot film data was input through Excel and MATLAB as described in the previous process, velocity data was normalized with respect to the freestream velocity, and position information was normalized with respect to the cylinder diameter. Each hot film was analyzed separate from other hot film. MATLAB's curve fitting function, ''cftool,'' was used to fit smooth curves to the velocity profiles [9]. A Fourier series was used as the curve fitting function.

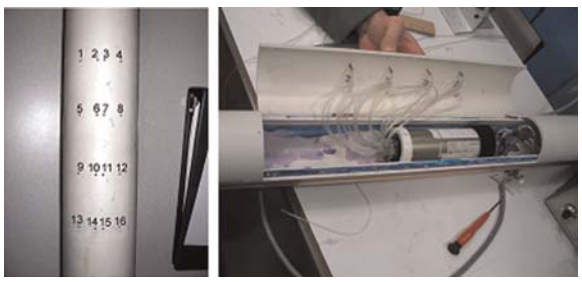

Figure 3 Pressure port locations and scanivalve pressure multiplexer. [Color figure can be viewed in the online issue, which is available at wileyonlinelibrary.com.]

RESULTS

Experimental Results and Validation of CFD Simulations

The effects of time step and grid on the simulation results are examined. Figure 4a shows the time history of the drag coefficient with two different grid resolutions and Figure 4b shows the effect of the time step on the simulation results. For these plots, the drag coefficient was calculated based on the drag force:

$$C_D = \frac{F_x}{(1/2)\rho U^2 A} \quad (1)$$

where U is the free stream velocity, ρ is the free stream density, and A is the frontal area. Figure 4 shows that the results are not completely grid-independent, but for flow fields with an absolute instability such as the cylinder wake, where are there

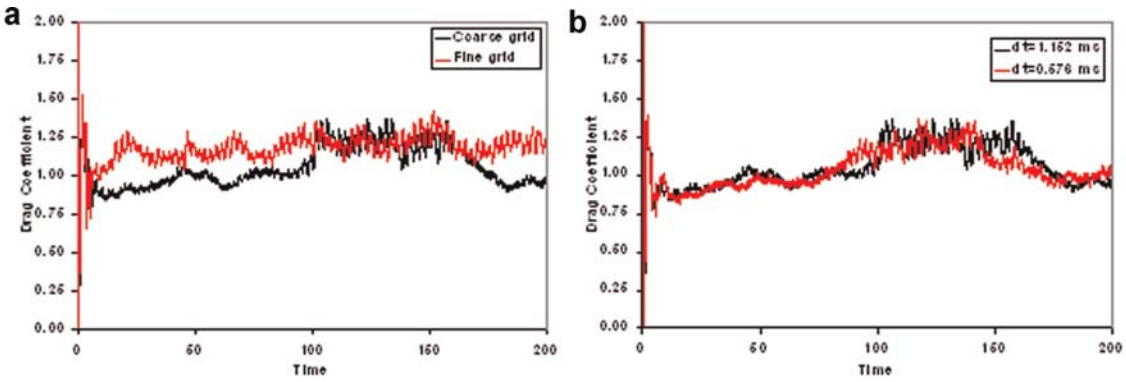

Figure 4 Comparison of drag coefficient time history. (a) Influence of grid resolution and (b) influence of time step. [Color figure can be viewed in the online issue, which is available at wileyonlinelibrary.com.]

are small scale fluctuations because of turbulence, a complete grid-independent solution is not expected.

To determine the pressure coefficients around the cylinder as a function of the angle (Θ) with the freestream, experimental data files are loaded into a self-programmed MATLAB file. The freestream velocities of the data files are plotted and analyzed. The velocities appear to be consistent throughout the data collection process. With the freestream velocities showing consistency, the surface pressure data obtained from the Baratron and Validyne sensors were loaded. The pressures at each cylinder surface location are time-averaged. With usable pressure and velocity data, the next step is to apply a filter to isolate the desired signals. The filter is the aforementioned Butterworth digital filter design. After the signals are filtered, the next step in the process is to develop an FFT of the signals to ensure the proper shedding frequency has been attained. Figure 5 shows the FFT graph with an expected peak just below 10 Hz for the freestream velocity of the tunnel.

Since the friction drag only constitutes approximately 3% of the total drag at a Reynolds number of $Re = 20{,}000$ based on

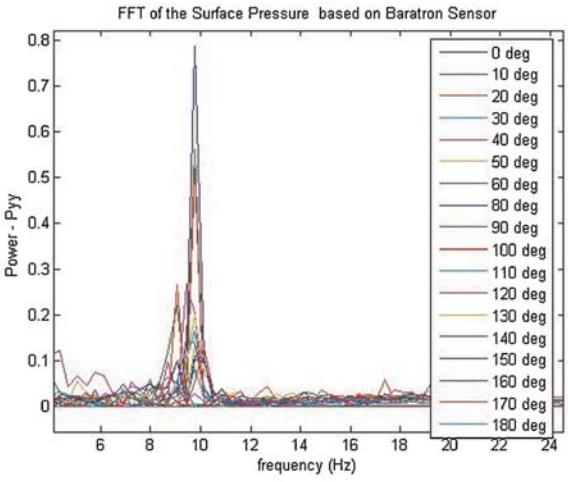

Figure 5 FFT of the surface pressure based on Baratron sensor. [Color figure can be viewed in the online issue, which is available at wileyonlinelibrary.com.]

theory, the average drag force was calculated based on the surface pressure measurements using:

$$C_{\mathrm{D}} = \frac{1}{2}\int_0^{2\pi} c_p \cos\theta \, \mathrm{d}\theta \tag{2}$$

where C_p is the surface pressure coefficient obtained from surface pressure values measured with 10° increments around the circumference of the cylinder, using:

$$C_p = \frac{P - P_\infty}{(1/2)\rho U^2} \tag{3}$$

where P is the static pressure and P_∞ is the freestream static pressure.

To evaluate the integral of the pressure coefficients to calculate the drag coefficient from the experiments, the trapezoidal rule is used. The trapezoidal rule simply divides the curve into small trapezoids and calculates the area [10]. The resultant values for the experimental results and the CFD analysis, as well as similar studies in literature are shown in Table 1. With the blockage corrections applied [11], the drag coefficient results from the wind tunnel testing correlate well with computational effort.

The time-averaged pressure coefficient on the center plane ($y/D = 2$) obtained from the computations and experiments as well as the results found in literature are shown in Figure 6. First, the two sensors used in the experiments, Validyne and Baratron are in good agreement with each other. When blockage correction is performed on wind tunnel data, the computations are in agreement with experiments where both of them show similar trends for pressure distribution. Pressure coefficient decreases at the point where the separation occurs in both of them.

Table 1 Comparison of Mean Drag Coefficient

Study	Mean CD
Computation-coarse grid	1.19
Computation-fine grid	1.20
Lim and Lee (2002) [13]	1.16
Anderson (1991) [14]	1.20
Experiment	1.19

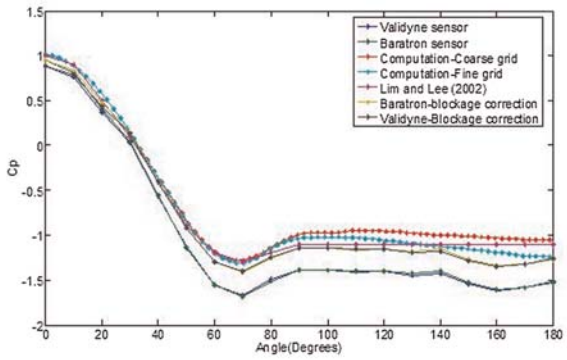

Figure 6 Time averaged surface pressure distribution on the center plane y/D = 2. [Color figure can be viewed in the online issue, which is available at wileyonlinelibrary.com.]

Time-averaged velocity information taken from hot films in the wake of the cylinder along with information gleaned from the computational study is illustrated in Figure 7. The velocity was non-dimensionalized with respect to freestream components of velocity. While the general shapes of all the curves match, information in Figure 7 indicates that the hot films are consistently measuring higher than expected wake velocities compared to the CFD analysis. The source of the error is speculated to lie within the hot film calibration, which is difficult to perform.

The Strouhal number was calculated using frequency information from the Baratron and Validyne pressure sensors as well as a hot film while velocity is gained from the LSWT pressure transducers. The Strouhal number, corrected for blockage, is displayed in Table 2. The Strouhal number obtained from the computational results is 0.2 which indicates strong correlation between the computational and experimental results.

Determination of the Region of Validity (Lock-In Region) for Plasma Actuators

Plasma forcing of the flow around the cylinder is used to create a lock-in region. The lock-in region is the region where the flow responds to the forcing frequency by adapting its shedding

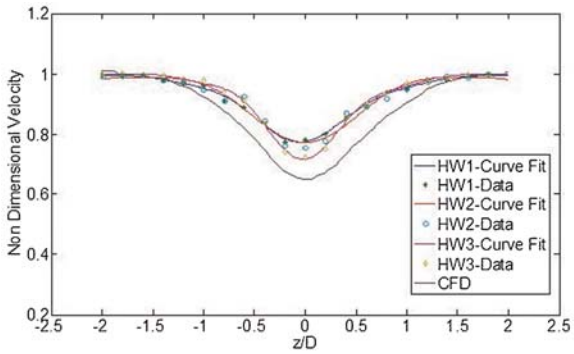

Figure 7 Cylinder lateral wake velocity profile. [Color figure can be viewed in the online issue, which is available at wileyonlinelibrary.com.]

Table 2 Comparison of Strouhal Number (St)

Method	Velocity (ft/s)	Frequency (Hz)	Strouhal number (experiment)
Baratron	14.29	9.78	0.19
Validyne	14.29	9.78	0.19
Hotwire	13.74	9.78	0.20
Computation	—	10	0.193

frequency to the actuator frequency. The forcing of plasma is sinusoidal in nature and is characterized by the non-dimensional frequency, based on the ratio of plasma actuation frequency to natural shedding frequency, f/f_0, and the plasma forcing amplitude (V). The forcing envelope is in the intervals, 1 kV < V < 16 kV and $0.7 < f/f_0 < 1.3$. Many forcing cases demonstrate either strong or weak lock-in. However, experimentation reveals that some cases on the border of the probable lock-in region show mixed behavior. Therefore, it is essential to determine exact criteria for lock-in qualification. The method of data reduction for this analysis is discussed at length in the post-processing section. A forcing case resulting in lock-in must fulfill two criteria. The power spectral density (PSD) analysis must reveal a minimum power level that is a suitable limit to decide if the frequency of the flow adjusts itself to the forcing frequency of plasma and it must have coherence between hot films and within a single hot film. The power level must be high enough to show that the flow adjusts itself according to the forcing frequency of the actuator if there is lock-in. The limit was set to be 0.04 based on observation. Based on these requirements, the shed vortices must exhibit spanwise and temporal coherence with a minimum frequency power level, which is based on the concept of the Welch averaged periodgram method, which, discussed previously, normalizes the FFT. This presents the FFT results independent of sample size and allows one to compare different data sets. Figure 8 is a representative case showing lock-in forcing close to the natural shedding frequency (9.8 Hz) using 11.01 kV of plasma for the four hotwire probes. Figure 8 indicates a strong tendency towards shedding vortices at the forced frequency. When the plasma forcing is applied, a dominant frequency exists at 10 Hz

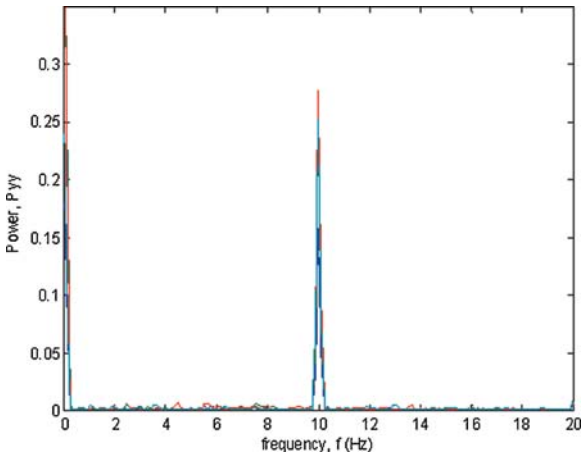

Figure 8 PSD of plasma forcing inside the lock-in region. [Color figure can be viewed in the online issue, which is available at wileyonlinelibrary.com.]

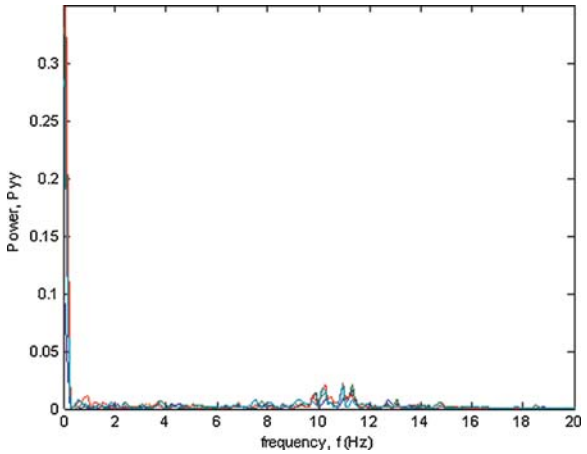

Figure 9 PSD of plasma forcing outside the lock-in region. [Color figure can be viewed in the online issue, which is available at wileyonlinelibrary.com.]

for all four hot films placed in the wake, and relatively little spectral power at any other frequencies. Due to the fact that forcing is applied relatively close to the natural shedding frequency at a high voltage, the resulting wake contains vortices which shed very predictably due to lock-in at the assigned actuation frequency.

Figure 9 depicts a forcing parameter set, 12 Hz and 11.01 kV, beyond the lock-in envelope. While the forcing voltage is the same as in Figure 8, the forcing frequency is 20% higher than that of the previous case, and therefore much higher than the natural shedding frequency. Figure 9 shows that there is some periodic behavior in the region between 10 and 12 Hz. However, the corresponding PSD values are very weak compared to the lock-in requirements, and are dispersed over a region of frequencies. This indicates that there is not a single, discrete value for forcing frequency with which the shed vortices are locking-in. This is a case where there is no lock-in. Many forcing cases used when developing a lock-in region are shown to have periodic behavior which lies in between these two extreme cases.

Constructed using the lock-in criteria, Figure 10 displays the overall results for the lock-in analysis. Figure 10 indicates that there is a triangle shaped lock-in envelope. The plot indicates a maximum range of lock-in, from $0.87f/f_0$ to $1.20f/f_0$, can be achieved at 14.7 kV. From there, the region decreases in size as the forcing voltage decreases. This general behavior appears to be consistent with previous experimental results of Blevin concerning lock-in at lower Reynolds numbers [12]. Both the current research effort and the previous research show that a wider range of lock-in is possible at higher forcing amplitudes.

Additionally, the current effort indicates that there may be a practical minimum voltage for lock-in. The lock-in region is very narrow at lower forcing voltages (<8 kV). The narrow area may be due to the fact that a minimum initial amount of voltage is required for any lock-in. Below this voltage, for this Reynolds number, achieving lock-in is not possible to a noticeable degree. Also, the lock-in region seems to pinch-off at the very top of the region.

CONCLUSIONS AND RECOMMENDATIONS

A computational fluid dynamics model, which is increasingly applicable to many different types of aerodynamic modeling, is shown to correlate strongly with experimental data for flow around a cylinder at a Reynolds number of 20,000. Surface pressures measured during experimental testing, Strouhal number, and the average drag coefficient show good agreement with the CFD model. Even though the wake velocity profile does not match computational data exactly, the source of the error is speculated to lie within the hot film calibration. This indicates that computational fluid dynamics may have great

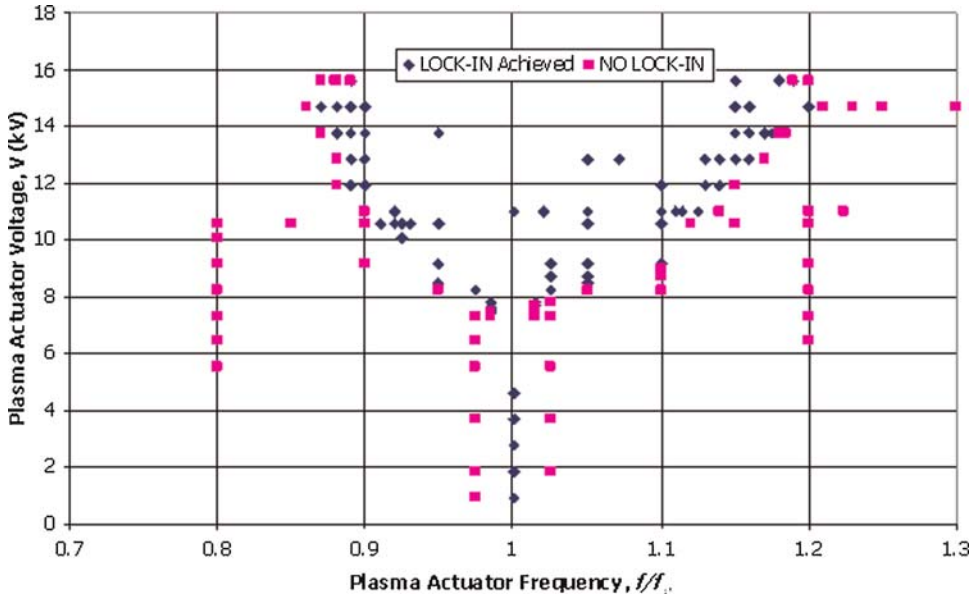

Figure 10 Lock-in envelope at Re = 20,000; z = −D/2. [Color figure can be viewed in the online issue, which is available at wileyonlinelibrary.com.]

applicability to continuing studies in cylinder wake feedback control. This is very important because it would allow researchers to study flow behavior without the constraints associated with actual wind tunnel testing. Additionally, results show that blockage corrections are an important step in post-processing to ensure accurate results. While many experiments may not have a great deal of blockage, factoring corrections into the data would increase the overall certainty of the results.

Experiments have shown that a lock-in region can be identified for plasma forcing at a Reynolds number of 20,000. As the plasma forcing amplitude (voltage) increases, the range of frequencies over which actuation can attain lock-in also increases, creating an upside-down, triangular envelope. The lock-in regime is shown to be asymmetrical with a larger region of lock-in observed at frequencies above natural shedding frequency of the flow, and further research is recommended to explore this phenomenon. This development needs to be examined more closely in future research. The next step is to incorporate plasma forcing to CFD simulations of the cylinder wake flow and validate this model using transient data. Additionally, as more confidence is gained in both the physical and computational models, the pressure sensors can be used exclusively in the design of a system to close the loop, providing active flow control to the system. Following an accurate high resolution simulation of a plasma-forced circular cylinder flow, within the lock-in region identified by these experiments, a low dimensional model will be developed for controller design.

The study is successful in combining fluid dynamics research with flow control crossing boundaries between engineering disciplines, as well as integrating experimentation with computational research for undergraduate education.

ACKNOWLEDGMENTS

The authors would like to thank USAFA cadets Brian Brown-Dymkoski and Dan Helland who performed this research and also like to thank AFOSR/Dynamics and Controls Directorate for their financial support. The contributions of SSgt Mary Church-O'Brien and Mr. Ken Ostasiewski were vital to the success of the data collection in the wind tunnel. The computational help from Dr. James Forsythe of Cobalt Solutions is also appreciated. All the CFD simulations were performed at US Air Force Academy, Blackbird cluster.

REFERENCES

[1] R. P. Feynman, R. Leighton, and M. Sands, The Feynman lectures in physics, 1st edition, Addison Wesley Longman, Boston, 1970.
[2] T. Von Kármán, The wind and beyond, Little, Brown and Company, Boston, MA, 1967.
[3] G. T. Taylor, R. L. Nudds, and A. L. R. Thomas, Flying and swimming animals cruise at a Strouhal number tuned for high power efficiency, Nature 425 (2003), 707−711.
[4] T. McLaughlin, B. Felker, J. Avery, and L. Enloe, Further Experiments in Cylinder Wake Modification with Dielectric Barrier Discharge Forcing, AIAA-2006-1409, January 2006.
[5] B. L. Snyder, J. A. Lewis, K. Cohen, C. A. Seaver, and T. McLaughlin, Closed Loop Plasma Active Control Technology (CLOPACT). Internal Report, Department of Aeronautics, United States Air Force Academy, May 2006.
[6] W. Z. Strang, R. F. Tomaro, and M. J. Grismer, The Defining Methods of Cobalt60: A Parallel, Implicit, Unstructured Euler/Navier Stokes Flow Solver, AIAA 99-0786, January 1999.
[7] R. Hansen and J. Forsythe, Large and Detached Eddy Simulations of a Circular Cylinder Using Unstructured Grids, AIAA-2003-775, January 2003.
[8] S. A. Morton, J. R. Forsythe, K. D. Squires, and K. E. Wurtzler, Assessment of Unstructured Grids For Detached Eddy Simulation of High Reynolds Number Separated Flows, Proceedings of the Eight International Conference on Numerical Grid Generation in Computational Field Simulations, 2002.
[9] The Mathworks, Curve fitting toolbox for use with MATLAB, User's Guide, Ver. 1, The MathWorks, Natick, Massachusetts, 2006.
[10] S. P. Chapra and R. P. Canale, Numerical methods for engineers, 3rd edition, McGraw Hill, New York, 1998.
[11] H. J. Allen and W. G. Vincenti, Wall interference in a two-dimensional-flow wind tunnel, with consideration of the effect of compressibility, NACA Report 782, 1944.
[12] R. D. Blevins, Flow induced vibration, 2nd edition, Von Nostrand Reinhold, New York, 1990, p. 54.
[13] J. D. Anderson, Fundamentals of aerodynamics, 2nd edition, McGraw-Hill, New York, 1991.
[14] H. Lim and S. Lee, Flow control of circular cylinders with longitudinal grooved surfaces, AIAA Jnl 40 (October 2002).

BIOGRAPHIES

Dr. Selin Aradag was born in Ankara, Turkey in 1979. She received her BS and MS degrees from METU, Department of Mechanical Engineering in Ankara in 2000 and 2002. She received her PhD in mechanical and aerospace engineering from Rutgers University in 2006. She worked for the US Air Force Academy for 2 years as a researcher after graduation. Her research interests are in the area of computational fluid dynamics, flow control and high speed flows. Currently, she is an assistant professor at TOBB University of Economics and Technology in Ankara. She teaches Fluid Mechanics, Thermodynamics and Thermal System Design courses.

Dr. Kelly Cohen, an associate professor of Aerospace Engineering, has been at the University of Cincinnati (UC) since 2007. He obtained his PhD in aerospace engineering at the Technion-Israel Institute of Technology in 1999. At UC, he teaches the following undergraduate courses: integrated aircraft engineering, fundamental control theory, and modeling and simulation of dynamic systems; as well as the following graduate courses: analytical dynamics, introduction to intelligent control, and optimal control. His research interests include: intelligent systems, cooperative multi-agent control, morphing aircraft, unmanned aerial vehicles, feedback flow control, low order modeling, and nonlinear system identification.

Christopher A. Seaver (Lt Col (ret)) was born on December 15, 1958 in Cincinnati, Ohio. He graduated from the United States Air Force May 1980 with a BS in aeronautical engineering. He received his MS in aeronautical engineering from the Air Force Institute of Technology at Wright-Patterson AFB, OH. He worked for the US Air Force as a pilot and instructor for several years. He worked as an assistant professor at US Air Force Academy, Department of Aeronautics teaching basic engineering, thermodynamics, and propulsion and retired in September 2006. He is currently the Deputy Director of Operations for the DFAN Aeronautics Laboratory.

Dr. Thomas McLaughlin is the Director of the Aeronautics Research Center at the U.S. Air Force Academy. He is also discipline director for the Department of Aeronautics' Experimental and Computational Investigations area, helping USAFA gain a reputation as a leader in integrating those investigation techniques. His 25-year engineering career spans a range of USAF engineering issues including nuclear hardening, precision pointing and tracking, and a number of aerodynamic and fluid dynamic issues. He has authored or co-authored over 100 publications in fields including unsteady aerodynamics, closed loop flow control, dielectric barrier plasma actuators, and aero-optics. He is an associate fellow of the American Institute of Aeronautics and Astronautics.